PHYSICAL REVIEW D **92,** 012008 (2015)

Search for the isospin violating decay $Y(4260) \to J/\psi\eta\pi^0$

M. Ablikim,[1] M. N. Achasov,[9,a] X. C. Ai,[1] O. Albayrak,[5] M. Albrecht,[4] D. J. Ambrose,[44] A. Amoroso,[48a,48c] F. F. An,[1] Q. An,[45] J. Z. Bai,[1] R. Baldini Ferroli,[20a] Y. Ban,[31] D. W. Bennett,[19] J. V. Bennett,[5] M. Bertani,[20a] D. Bettoni,[21a] J. M. Bian,[43] F. Bianchi,[48a,48c] E. Boger,[23,h] O. Bondarenko,[25] I. Boyko,[23] R. A. Briere,[5] H. Cai,[50] X. Cai,[1] O. Cakir,[40a,b] A. Calcaterra,[20a] G. F. Cao,[1] S. A. Cetin,[40b] J. F. Chang,[1] G. Chelkov,[23,c] G. Chen,[1] H. S. Chen,[1] H. Y. Chen,[2] J. C. Chen,[1] M. L. Chen,[1] S. J. Chen,[29] X. Chen,[1] X. R. Chen,[26] Y. B. Chen,[1] H. P. Cheng,[17] X. K. Chu,[31] G. Cibinetto,[21a] D. Cronin-Hennessy,[43] H. L. Dai,[1] J. P. Dai,[34] A. Dbeyssi,[14] D. Dedovich,[23] Z. Y. Deng,[1] A. Denig,[22] I. Denysenko,[23] M. Destefanis,[48a,48c] F. De Mori,[48a,48c] Y. Ding,[27] C. Dong,[30] J. Dong,[1] L. Y. Dong,[1] M. Y. Dong,[1] S. X. Du,[52] P. F. Duan,[1] J. Z. Fan,[39] J. Fang,[1] S. S. Fang,[1] X. Fang,[45] Y. Fang,[1] L. Fava,[48b,48c] F. Feldbauer,[22] G. Felici,[20a] C. Q. Feng,[45] E. Fioravanti,[21a] M. Fritsch,[14,22] C. D. Fu,[1] Q. Gao,[1] X. Y. Gao,[2] Y. Gao,[39] Z. Gao,[45] I. Garzia,[21a] C. Geng,[45] K. Goetzen,[10] W. X. Gong,[1] W. Gradl,[22] M. Greco,[48a,48c] M. H. Gu,[1] Y. T. Gu,[12] Y. H. Guan,[1] A. Q. Guo,[1] L. B. Guo,[28] Y. Guo,[1] Y. P. Guo,[22] Z. Haddadi,[25] A. Hafner,[22] S. Han,[50] Y. L. Han,[1] X. Q. Hao,[15] F. A. Harris,[42] K. L. He,[1] Z. Y. He,[30] T. Held,[4] Y. K. Heng,[1] Z. L. Hou,[1] C. Hu,[28] H. M. Hu,[1] J. F. Hu,[48a,48c] T. Hu,[1] Y. Hu,[1] G. M. Huang,[6] G. S. Huang,[45] H. P. Huang,[50] J. S. Huang,[15] X. T. Huang,[33] Y. Huang,[29] T. Hussain,[47] Q. Ji,[1] Q. P. Ji,[30] X. B. Ji,[1] X. L. Ji,[1] L. L. Jiang,[1] L. W. Jiang,[50] X. S. Jiang,[1] J. B. Jiao,[33] Z. Jiao,[17] D. P. Jin,[1] S. Jin,[1] T. Johansson,[49] A. Julin,[43] N. Kalantar-Nayestanaki,[25] X. L. Kang,[1] X. S. Kang,[30] M. Kavatsyuk,[25] B. C. Ke,[5] R. Kliemt,[14] B. Kloss,[22] O. B. Kolcu,[40b,d] B. Kopf,[4] M. Kornicer,[42] W. Kühn,[24] A. Kupsc,[49] W. Lai,[1] J. S. Lange,[24] M. Lara,[19] P. Larin,[14] C. Leng,[48c] C. H. Li,[1] Cheng Li,[45] D. M. Li,[52] F. Li,[1] G. Li,[1] H. B. Li,[1] J. C. Li,[1] Jin Li,[32] K. Li,[13] K. Li,[33] Lei Li,[3] P. R. Li,[41] T. Li,[33] W. D. Li,[1] W. G. Li,[1] X. L. Li,[33] X. M. Li,[12] X. N. Li,[1] X. Q. Li,[30] Z. B. Li,[38] H. Liang,[45] Y. F. Liang,[36] Y. T. Liang,[24] G. R. Liao,[11] D. X. Lin,[14] B. J. Liu,[1] C. X. Liu,[1] F. H. Liu,[35] Fang Liu,[1] Feng Liu,[6] H. B. Liu,[12] H. H. Liu,[1] H. H. Liu,[16] H. M. Liu,[1] J. Liu,[1] J. P. Liu,[50] J. Y. Liu,[1] K. Liu,[39] K. Y. Liu,[27] L. D. Liu,[31] P. L. Liu,[1] Q. Liu,[41] S. B. Liu,[45] X. Liu,[26] X. X. Liu,[41] Y. B. Liu,[30] Z. A. Liu,[1] Zhiqiang Liu,[1] Zhiqing Liu,[22] H. Loehner,[25] X. C. Lou,[1,e] H. J. Lu,[17] J. G. Lu,[1] R. Q. Lu,[18] Y. Lu,[1] Y. P. Lu,[1] C. L. Luo,[28] M. X. Luo,[51] T. Luo,[42] X. L. Luo,[1] M. Lv,[1] X. R. Lyu,[41] F. C. Ma,[27] H. L. Ma,[1] L. L. Ma,[33] Q. M. Ma,[1] S. Ma,[1] T. Ma,[1] X. N. Ma,[30] X. Y. Ma,[1] F. E. Maas,[14] M. Maggiora,[48a,48c] Q. A. Malik,[47] Y. J. Mao,[31] Z. P. Mao,[1] S. Marcello,[48a,48c] J. G. Messchendorp,[25] J. Min,[1] T. J. Min,[1] R. E. Mitchell,[19] X. H. Mo,[1] Y. J. Mo,[6] C. Morales Morales,[14] K. Moriya,[19] N. Yu. Muchnoi,[9,a] H. Muramatsu,[43] Y. Nefedov,[23] F. Nerling,[14] I. B. Nikolaev,[9,a] Z. Ning,[1] S. Nisar,[8] S. L. Niu,[1] X. Y. Niu,[1] S. L. Olsen,[32] Q. Ouyang,[1] S. Pacetti,[20b] P. Patteri,[20a] M. Pelizaeus,[4] H. P. Peng,[45] K. Peters,[10] J. Pettersson,[49] J. L. Ping,[28] R. G. Ping,[1] R. Poling,[43] Y. N. Pu,[18] M. Qi,[29] S. Qian,[1] C. F. Qiao,[41] L. Q. Qin,[33] N. Qin,[50] X. S. Qin,[1] Y. Qin,[31] Z. H. Qin,[1] J. F. Qiu,[1] K. H. Rashid,[47] C. F. Redmer,[22] H. L. Ren,[18] M. Ripka,[22] G. Rong,[1] X. D. Ruan,[12] V. Santoro,[21a] A. Sarantsev,[23,f] M. Savrié,[21b] K. Schoenning,[49] S. Schumann,[22] W. Shan,[31] M. Shao,[45] C. P. Shen,[2] P. X. Shen,[30] X. Y. Shen,[1] H. Y. Sheng,[1] W. M. Song,[1] X. Y. Song,[1] S. Sosio,[48a,48c] S. Spataro,[48a,48c] G. X. Sun,[1] J. F. Sun,[15] S. S. Sun,[1] Y. J. Sun,[45] Y. Z. Sun,[1] Z. J. Sun,[1] Z. T. Sun,[19] C. J. Tang,[36] X. Tang,[1] I. Tapan,[40c] E. H. Thorndike,[44] M. Tiemens,[25] D. Toth,[43] M. Ullrich,[24] I. Uman,[40b] G. S. Varner,[42] B. Wang,[30] B. L. Wang,[41] D. Wang,[31] D. Y. Wang,[31] K. Wang,[1] L. L. Wang,[1] L. S. Wang,[1] M. Wang,[33] P. Wang,[1] P. L. Wang,[1] Q. J. Wang,[1] S. G. Wang,[31] W. Wang,[1] X. F. Wang,[39] Y. D. Wang,[20a] Y. F. Wang,[1] Y. Q. Wang,[22] Z. Wang,[1] Z. G. Wang,[1] Z. H. Wang,[45] Z. Y. Wang,[1] T. Weber,[22] D. H. Wei,[11] J. B. Wei,[31] P. Weidenkaff,[22] S. P. Wen,[1] U. Wiedner,[4] M. Wolke,[49] L. H. Wu,[1] Z. Wu,[1] L. G. Xia,[39] Y. Xia,[18] D. Xiao,[1] Z. J. Xiao,[28] Y. G. Xie,[1] Q. L. Xiu,[1] G. F. Xu,[1] L. Xu,[1] Q. J. Xu,[13] Q. N. Xu,[41] X. P. Xu,[37] L. Yan,[45] W. B. Yan,[45] W. C. Yan,[45] Y. H. Yan,[18] H. X. Yang,[1] L. Yang,[50] Y. Yang,[6] Y. X. Yang,[11] H. Ye,[1] M. Ye,[1] M. H. Ye,[7] J. H. Yin,[1] B. X. Yu,[1] C. X. Yu,[30] H. W. Yu,[31] J. S. Yu,[26] C. Z. Yuan,[1] W. L. Yuan,[29] Y. Yuan,[1] A. Yuncu,[40b,g] A. A. Zafar,[47] A. Zallo,[20a] Y. Zeng,[18] B. X. Zhang,[1] B. Y. Zhang,[1] C. Zhang,[29] C. C. Zhang,[1] D. H. Zhang,[1] H. H. Zhang,[38] H. Y. Zhang,[1] J. J. Zhang,[1] J. L. Zhang,[1] J. Q. Zhang,[1] J. W. Zhang,[1] J. Y. Zhang,[1] J. Z. Zhang,[1] K. Zhang,[1] L. Zhang,[1] S. H. Zhang,[1] X. Y. Zhang,[33] Y. Zhang,[1] Y. H. Zhang,[1] Y. T. Zhang,[45] Z. H. Zhang,[6] Z. P. Zhang,[45] Z. Y. Zhang,[50] G. Zhao,[1] J. W. Zhao,[1] J. Y. Zhao,[1] J. Z. Zhao,[1] Lei Zhao,[45] Ling Zhao,[1] M. G. Zhao,[30] Q. Zhao,[1] Q. W. Zhao,[1] S. J. Zhao,[52] T. C. Zhao,[1] Y. B. Zhao,[1] Z. G. Zhao,[45] A. Zhemchugov,[23,h] B. Zheng,[46] J. P. Zheng,[1] W. J. Zheng,[33] Y. H. Zheng,[41] B. Zhong,[28] L. Zhou,[1] Li Zhou,[30] X. Zhou,[50] X. K. Zhou,[45] X. R. Zhou,[45] X. Y. Zhou,[1] K. Zhu,[1] K. J. Zhu,[1] S. Zhu,[1] X. L. Zhu,[39] Y. C. Zhu,[45] Y. S. Zhu,[1] Z. A. Zhu,[1] J. Zhuang,[1] L. Zotti,[48a,48c] B. S. Zou,[1] and J. H. Zou[1]

(BESIII Collaboration)

[1]*Institute of High Energy Physics, Beijing 100049, People's Republic of China*
[2]*Beihang University, Beijing 100191, People's Republic of China*
[3]*Beijing Institute of Petrochemical Technology, Beijing 102617, People's Republic of China*
[4]*Bochum Ruhr-University, D-44780 Bochum, Germany*
[5]*Carnegie Mellon University, Pittsburgh, Pennsylvania 15213, USA*
[6]*Central China Normal University, Wuhan 430079, People's Republic of China*
[7]*China Center of Advanced Science and Technology, Beijing 100190, People's Republic of China*
[8]*COMSATS Institute of Information Technology, Lahore, Defence Road, Off Raiwind Road, 54000 Lahore, Pakistan*
[9]*G.I. Budker Institute of Nuclear Physics SB RAS (BINP), Novosibirsk 630090, Russia*
[10]*GSI Helmholtzcentre for Heavy Ion Research GmbH, D-64291 Darmstadt, Germany*
[11]*Guangxi Normal University, Guilin 541004, People's Republic of China*
[12]*GuangXi University, Nanning 530004, People's Republic of China*
[13]*Hangzhou Normal University, Hangzhou 310036, People's Republic of China*
[14]*Helmholtz Institute Mainz, Johann-Joachim-Becher-Weg 45, D-55099 Mainz, Germany*
[15]*Henan Normal University, Xinxiang 453007, People's Republic of China*
[16]*Henan University of Science and Technology, Luoyang 471003, People's Republic of China*
[17]*Huangshan College, Huangshan 245000, People's Republic of China*
[18]*Hunan University, Changsha 410082, People's Republic of China*
[19]*Indiana University, Bloomington, Indiana 47405, USA*
[20a]*INFN Laboratori Nazionali di Frascati, I-00044, Frascati, Italy*
[20b]*INFN and University of Perugia, I-06100, Perugia, Italy*
[21a]*INFN Sezione di Ferrara, I-44122, Ferrara, Italy*
[21b]*University of Ferrara, I-44122, Ferrara, Italy*
[22]*Johannes Gutenberg University of Mainz, Johann-Joachim-Becher-Weg 45, D-55099 Mainz, Germany*
[23]*Joint Institute for Nuclear Research, 141980 Dubna, Moscow region, Russia*
[24]*Justus Liebig University Giessen, II. Physikalisches Institut, Heinrich-Buff-Ring 16, D-35392 Giessen, Germany*
[25]*KVI-CART, University of Groningen, NL-9747 AA Groningen, Netherlands*
[26]*Lanzhou University, Lanzhou 730000, People's Republic of China*
[27]*Liaoning University, Shenyang 110036, People's Republic of China*
[28]*Nanjing Normal University, Nanjing 210023, People's Republic of China*
[29]*Nanjing University, Nanjing 210093, People's Republic of China*
[30]*Nankai University, Tianjin 300071, People's Republic of China*
[31]*Peking University, Beijing 100871, People's Republic of China*
[32]*Seoul National University, Seoul, 151-747 Korea*
[33]*Shandong University, Jinan 250100, People's Republic of China*
[34]*Shanghai Jiao Tong University, Shanghai 200240, People's Republic of China*
[35]*Shanxi University, Taiyuan 030006, People's Republic of China*
[36]*Sichuan University, Chengdu 610064, People's Republic of China*
[37]*Soochow University, Suzhou 215006, People's Republic of China*
[38]*Sun Yat-Sen University, Guangzhou 510275, People's Republic of China*
[39]*Tsinghua University, Beijing 100084, People's Republic of China*
[40a]*Istanbul Aydin University, 34295 Sefakoy, Istanbul, Turkey*
[40b]*Dogus University, 34722 Istanbul, Turkey*
[40c]*Uludag University, 16059 Bursa, Turkey*
[41]*University of Chinese Academy of Sciences, Beijing 100049, People's Republic of China*
[42]*University of Hawaii, Honolulu, Hawaii 96822, USA*
[43]*University of Minnesota, Minneapolis, Minnesota 55455, USA*
[44]*University of Rochester, Rochester, New York 14627, USA*
[45]*University of Science and Technology of China, Hefei 230026, People's Republic of China*
[46]*University of South China, Hengyang 421001, People's Republic of China*
[47]*University of the Punjab, Lahore-54590, Pakistan*
[48a]*University of Turin, I-10125, Turin, Italy*
[48b]*University of Eastern Piedmont, I-15121, Alessandria, Italy*
[48c]*INFN, I-10125 Turin, Italy*
[49]*Uppsala University, Box 516, SE-75120 Uppsala, Sweden*

[50]Wuhan University, Wuhan 430072, People's Republic of China
[51]Zhejiang University, Hangzhou 310027, People's Republic of China
[52]Zhengzhou University, Zhengzhou 450001, People's Republic of China
(Received 4 May 2015; published 17 July 2015)

Using data samples collected at center-of-mass energies of $\sqrt{s} = 4.009$, 4.226, 4.257, 4.358, 4.416, and 4.599 GeV with the BESIII detector operating at the BEPCII storage ring, we search for the isospin violating decay $Y(4260) \to J/\psi\eta\pi^0$. No signal is observed, and upper limits on the cross section $\sigma(e^+e^- \to J/\psi\eta\pi^0)$ at the 90% confidence level are determined to be 3.6, 1.7, 2.4, 1.4, 0.9, and 1.9 pb, respectively.

DOI: 10.1103/PhysRevD.92.012008 PACS numbers: 14.40.Rt, 13.20.Gd, 13.66.Bc, 14.40.Pq

I. INTRODUCTION

The $Y(4260)$ charmoniumlike state was first observed in its decay to $\pi^+\pi^- J/\psi$ [1] and has a small coupling to open charm decay modes [2]. $Y(4260)$ is a vector ($J^{PC} = 1^{--}$) state that is only barely observable as an s-channel resonance in e^+e^- collisions and that appears at an energy where no conventional charmonium state is expected. Since its discovery, many theoretical studies have been carried out considering the $Y(4260)$ as a tetraquark state [3], D_1D or D_0D^* hadronic molecule [4], hybrid charmonium [5], baryonium state [6], etc.

Recently, in the study of $Y(4260) \to \pi^+\pi^- J/\psi$, a charged charmoniumlike structure, the $Z_c(3900)^{\pm}$, was observed in the $\pi^{\pm} J/\psi$ invariant mass spectrum by the BESIII [7] and Belle experiments [8] and confirmed shortly thereafter with CLEO-c data [9]. In the molecule model [10], the $Y(4260)$ is proposed to have a large $D_1\bar{D}$ component, while $Z_c(3900)^{\pm}$ has a $D\bar{D}^*$ component.

BESIII recently reported the observation of $e^+e^- \to \gamma X(3872) \to \gamma\pi^+\pi^- J/\psi$ [11]. The cross section measurements strongly support the existence of the radiative transition $Y(4260) \to \gamma X(3872)$. One significant feature of the $X(3872)$ that differs from conventional charmonium is that the decay branching fraction of $X(3872)$ to $\pi^+\pi^-\pi^0 J/\psi$ is comparable to $\pi^+\pi^- J/\psi$ [12,13], so the isospin violating process occurs on a large scale.

Isospin violating decays can be used to probe the nature of heavy quarkonium. The hadro-charmonium model [14] and tetraquark models [15,16] predict that the reaction $\Upsilon(5S) \to \eta\pi^0$+bottomonium should be observable. The tetraquark model [17] also predicts that Z_c^0 can be produced in $Y(4260) \to J/\psi\eta\pi^0$ with Z_c^0 decaying into $J/\psi\pi^0$ and possibly $J/\psi\eta$ in the presence of sizable isospin violation. The molecular model [18] predicts a peak in the cross section of $Y(4260) \to J/\psi\eta\pi^0$ at the $D_1\bar{D}$ threshold and a narrow peak in the $J/\psi\eta$ invariant mass spectrum at the $D\bar{D}^*$ threshold.

In this paper, we present results on a search for the isospin violating decay $Y(4260) \to J/\psi\eta\pi^0$, with $J/\psi \to e^+e^-/\mu^+\mu^-$, $\pi^0 \to \gamma\gamma$, and $\eta \to \gamma\gamma$ (the other decay modes of η are not used due to much lower detection efficiency and branching fraction), based on e^+e^- annihilation data collected with the BESIII detector operating at the BEPCII storage ring [19] at center-of-mass energies of $\sqrt{s} = 4.009$, 4.226, 4.257, 4.358, 4.416, and 4.599 GeV.

II. BESIII DETECTOR AND MONTE CARLO SIMULATION

The BESIII detector, described in detail in Ref. [19], has a geometrical acceptance of 93% of 4π. A small-cell helium-based main drift chamber (MDC) provides a charged particle momentum resolution of 0.5% at 1 GeV/c in a 1 T magnetic field and supplies energy-loss (dE/dx) measurements with a resolution of 6% for minimum-ionizing pions. The electromagnetic calorimeter (EMC) measures photon energies with a resolution of 2.5% (5%) at 1.0 GeV in the barrel (end caps). Particle identification is provided by a time-of-flight system with a time resolution of 80 ps (110 ps) for the barrel (end caps). The muon system (MUC), located in the iron flux return yoke of the magnet, provides 2 cm position resolution and detects muon tracks with momentum greater than 0.5 GeV/c.

The GEANT4-based [20] Monte Carlo (MC) simulation software BOOST [21] includes the geometric description of the BESIII detector and a simulation of the detector response. It is used to optimize event selection criteria, estimate backgrounds, and evaluate the detection efficiency. For each energy point, we generate large signal MC samples of $e^+e^- \to J/\psi\eta\pi^0$, $J/\psi \to e^+e^-/\mu^+\mu^-$,

[a]Also at the Novosibirsk State University, Novosibirsk, 630090, Russia.
[b]Also at Ankara University, 06100 Tandogan, Ankara, Turkey.
[c]Also at the Moscow Institute of Physics and Technology, Moscow 141700, Russia and at the Functional Electronics Laboratory, Tomsk State University, Tomsk, 634050, Russia.
[d]Currently at Istanbul Arel University, 34295 Istanbul, Turkey.
[e]Also at University of Texas at Dallas, Richardson, Texas 75083, USA.
[f]Also at the NRC "Kurchatov Institute," PNPI, 188300, Gatchina, Russia.
[g]Also at Bogazici University, 34342 Istanbul, Turkey.
[h]Also at the Moscow Institute of Physics and Technology, Moscow 141700, Russia.

$\eta \to \gamma\gamma$, and $\pi^0 \to \gamma\gamma$ uniformly in phase space. Effects of initial state radiation (ISR) are simulated with KKMC [22], where the Born cross section of $e^+e^- \to J/\psi\eta\pi^0$ is assumed to follow a $Y(4260)$ Breit–Wigner line shape with resonance parameters taken from the Particle Data Group (PDG) [23]. Final state radiation effects associated with charged particles are handled with PHOTOS [24].

To study possible backgrounds, a MC sample of inclusive $Y(4260)$ decays, equivalent to an integrated luminosity of 825.6 pb^{-1}, is also generated at $\sqrt{s} = 4.260$ GeV. In these simulations, the $Y(4260)$ is allowed to decay generically, with the main known decay channels being generated using EVTGEN [25] with branching fractions set to world average values [23]. The remaining events associated with charmonium decays are generated with LUNDCHARM [26], while continuum hadronic events are generated with PYTHIA [27]. QED events ($e^+e^- \to e^+e^-$, $\mu^+\mu^-$, and $\gamma\gamma$) are generated with KKMC [22]. Backgrounds at other energy points are expected to be similar.

III. EVENT SELECTION

Events with two charged tracks with a net charge of zero are selected. For each good charged track, the polar angle in the MDC must satisfy $|\cos\theta| < 0.93$, and the point of closest approach to the e^+e^- interaction point must be within ± 10 cm in the beam direction and within ± 1 cm in the plane perpendicular to the beam direction. The momenta of leptons from the J/ψ decays in the laboratory frame are required to be larger than 1.0 GeV/c. E/p is used to separate electrons from muons, where E is the energy deposited in the EMC and p is the momentum measured by the MDC. For electron candidates, E/p should be larger than 0.7, while for muons, it should be less than 0.3. To suppress background from events with pion tracks in the final state, at least one of the two muons is required to have at least five layers with valid hits in the MUC.

Showers identified as photon candidates must satisfy fiducial and shower quality as well as timing requirements. The minimum EMC energy is 25 MeV for barrel showers ($|\cos\theta| < 0.80$) and 50 MeV for end cap showers ($0.86 < |\cos\theta| < 0.92$). To eliminate showers produced by charged particles, a photon must be separated by at least 5 deg from any charged track. The time information from the EMC is also used to suppress electronic noise and energy deposits unrelated to the event. At least four good photon candidates in each event are required.

To improve the momentum resolution and reduce the background, the event is subjected to a four-constraint (4C) kinematic fit under the hypothesis $e^+e^- \to \gamma\gamma\gamma\gamma l^+l^-(l = e/\mu)$, and the χ^2 is required to be less than 40. For events with more than four photons, the four photons with the smallest χ^2 from the 4C fit are assigned as the photons from η and π^0.

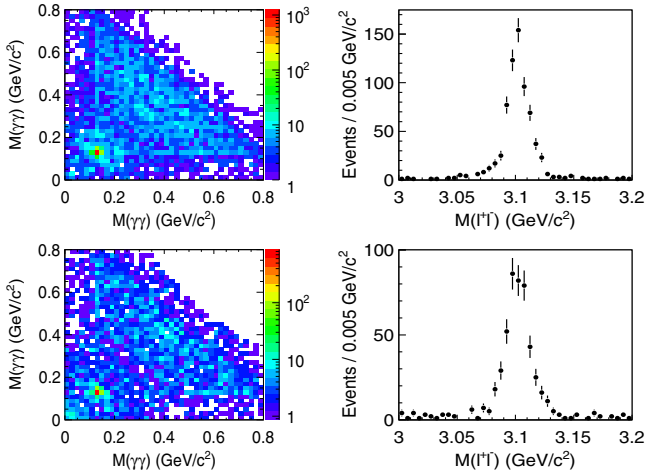

FIG. 1 (color online). Scatter plot of $M(\gamma\gamma)$ with all six combinations for events in the J/ψ signal region (left) and distribution of $M(l^+l^-)$ for events in the $\pi^0\pi^0$ signal region (right) for data at $\sqrt{s} = 4.226$ GeV (top) and 4.257 GeV (bottom).

After selecting the $\gamma\gamma\gamma\gamma l^+l^-$ candidate, scatter plots of $M(\gamma\gamma)$ with all six combinations of photon pairs for events in the J/ψ signal region ($3.067 < M(l^+l^-) < 3.127$ GeV/c^2) for data at $\sqrt{s} = 4.226$ and 4.257 GeV are shown in the left two panels of Fig. 1. Distributions of $M(l^+l^-)$ for events in the $\pi^0\pi^0$ signal region (both photon pairs satisfy $|M(\gamma\gamma) - m_{\pi^0}| < 10$ MeV/c^2) for data at $\sqrt{s} = 4.226$ and 4.257 GeV are shown in the right two panels of Fig. 1. Clear J/ψ peaks are observed, corresponding to $\pi^0\pi^0 J/\psi$ events. To remove this $\pi^0\pi^0 J/\psi$ background, events with any combination of photon pairs in the $\pi^0\pi^0$ region of the scatter plot are rejected.

After rejecting the $\pi^0\pi^0 J/\psi$ background, we choose the combination of photon pairs closest to the $\eta\pi^0$ signal region by minimizing $\sqrt{|\frac{M(\gamma_1\gamma_2)-m_\eta}{\sigma_\eta}|^2 + |\frac{M(\gamma_3\gamma_4)-m_{\pi^0}}{\sigma_{\pi^0}}|^2}$, where σ_η and σ_{π^0} are the η and π^0 resolutions obtained from the signal MC, respectively. The scatter plots of $M(\gamma\gamma)$ with the combination closest to the $\eta\pi^0$ signal region for events in the J/ψ signal region for data at $\sqrt{s} = 4.226$ and 4.257 GeV are shown in the top two panels of Fig. 2. No cluster of $\eta\pi^0$ events is observed in the J/ψ signal region, with a vertical band for $\pi^0 \to \gamma\gamma$ clearly visible, but no prominent band for $\eta \to \gamma\gamma$ is observed. The projections of the scatter plots on $M(\gamma_1\gamma_2)$ with $M(\gamma_3\gamma_4)$ in the π^0 signal region ($|M(\gamma_3\gamma_4) - m_{\pi^0}| < 10$ MeV/c^2) and projections on $M(\gamma_3\gamma_4)$ with $M(\gamma_1\gamma_2)$ in the η signal region ($|M(\gamma_1\gamma_2) - m_\eta| < 30$ MeV/c^2) for data are shown in the middle and bottom panels of Fig. 2, respectively.

The background for $e^+e^- \to J/\psi\eta\pi^0$ is studied using the inclusive MC sample at $\sqrt{s} = 4.260$ GeV. After imposing all event selection requirements, there are two background

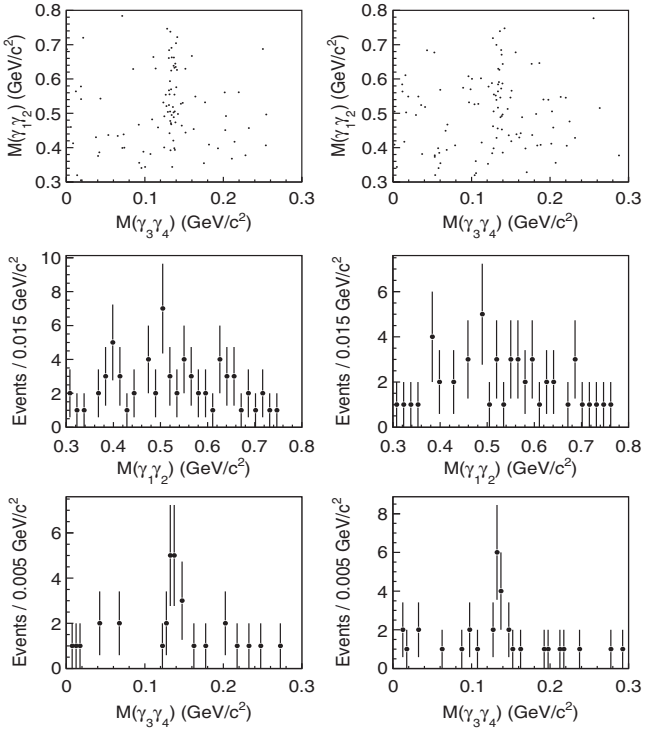

FIG. 2. Scatter plot of $M(\gamma\gamma)$ for the combination closest to the $\eta\pi^0$ signal region for events in the J/ψ signal region (top), projection of the scatter plot on $M(\gamma_1\gamma_2)$ with $M(\gamma_3\gamma_4)$ in π^0 signal region (middle), and projection of the scatter plot on $M(\gamma_3\gamma_4)$ with $M(\gamma_1\gamma_2)$ in η signal region (bottom) for data at $\sqrt{s} = 4.226$ GeV (left) and 4.257 GeV (right).

events from $e^+e^- \to \pi^0\pi^0 J/\psi$ and nine background events arising from $e^+e^- \to \gamma_{\rm ISR}\psi'$, $\gamma_{\rm ISR}\psi''$, and $\gamma_{\rm ISR}\psi(4040)$. No other background survives. The background can be evaluated with $\eta\pi^0$ sideband events. Distributions of $M(l^+l^-)$ for events in the $\eta\pi^0$ signal region for data at $\sqrt{s} = 4.226$ and 4.257 GeV are shown in Fig. 3. Distributions of $M(l^+l^-)$ for events corresponding to the normalized two-dimensional $\eta\pi^0$ sidebands are shown as shaded

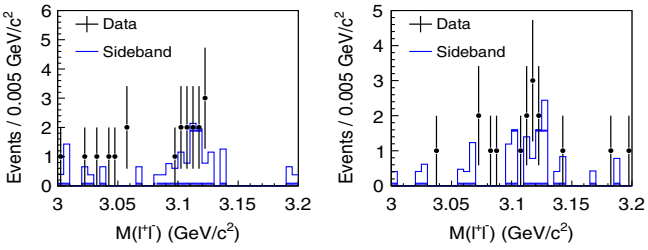

FIG. 3 (color online). Distributions of $M(l^+l^-)$ for events in $\eta\pi^0$ signal region and sideband regions for data at $\sqrt{s} = 4.226$ GeV (left) and 4.257 GeV (right). The error bars are the $M(l^+l^-)$ distributions for events in the $\eta\pi^0$ signal region, and the shaded histograms are those in the $\eta\pi^0$ sideband regions.

histograms. The η sideband regions are defined as $0.3978 < M(\gamma_1\gamma_2) < 0.4578$ GeV/c^2 and $0.6378 < M(\gamma_1\gamma_2) < 0.6978$ GeV/c^2. The π^0 sideband regions are defined as $0.0849 < M(\gamma_3\gamma_4) < 0.1049$ GeV/c^2 and $0.1649 < M(\gamma_3\gamma_4) < 0.1849$ GeV/c^2. The counted number of observed events in the $J/\psi\eta\pi^0$ signal region $N^{\rm obs}$ and number of background events estimated from $\eta\pi^0$ sidebands $N^{\rm bkg}$ are listed in Table I.

IV. CROSS SECTION UPPER LIMITS

Since no $J/\psi\eta\pi^0$ signal above the background is observed, upper limits on the Born cross section of $e^+e^- \to J/\psi\eta\pi^0$ at the 90% C.L. are determined using the formula

$$\sigma^{\rm Born} < \frac{N^{\rm up}_{\rm observed}}{\mathcal{L}(1+\delta^r)(1+\delta^v)(\epsilon^{ee}\mathcal{B}^{ee} + \epsilon^{\mu\mu}\mathcal{B}^{\mu\mu})\mathcal{B}^{\pi^0}\mathcal{B}^{\eta}}, \quad (1)$$

where $N^{\rm up}_{\rm observed}$ is the upper limit on the number of signal events; $\mathcal{L}$ is the integrated luminosity; $(1+\delta^r)$ is the radiative correction factor, which is taken from a QED calculation assuming the $e^+e^- \to J/\psi\eta\pi^0$ cross section is described by a $Y(4260)$ Breit–Wigner line shape with parameters taken from the PDG [23]; $(1+\delta^v)$ is the vacuum polarization factor including leptonic and hadronic parts and taken from a QED calculation with an accuracy of 0.5% [28]; ϵ^{ee} and $\epsilon^{\mu\mu}$ are the efficiencies for e^+e^- and $\mu^+\mu^-$ modes, respectively; $\mathcal{B}^{ee}$ and $\mathcal{B}^{\mu\mu}$ are the branching fractions of $J/\psi \to e^+e^-$ and $J/\psi \to \mu^+\mu^-$ [23], respectively; and $\mathcal{B}^{\eta}$ and $\mathcal{B}^{\pi^0}$ are the branching fractions of $\eta \to \gamma\gamma$ and $\pi^0 \to \gamma\gamma$ [23], respectively.

The efficiency corrected upper limit on the number of signal events $N^{\rm up} \equiv \frac{N^{\rm up}_{\rm observed}}{\epsilon^{ee}\mathcal{B}^{ee}+\epsilon^{\mu\mu}\mathcal{B}^{\mu\mu}}$ is estimated with $N^{\rm obs}$ and $N^{\rm bkg}$ using the profile likelihood method, which is implemented by TRolke in the ROOT framework [29]. The calculation for obtaining N^{up} includes the background fluctuation and the systematic uncertainty of the cross section measurement. The background fluctuation is assumed to follow a Poisson distribution. The systematic uncertainty of the cross section is taken as a Gaussian uncertainty.

The systematic uncertainty of the cross section measurement in Eq. (1) includes the luminosity measurement, detection efficiency, and intermediate decay branching fractions. The systematic uncertainties of the luminosity, track reconstruction, and photon detection are 1.0% [11], 1.0% per track [30], and 1.0% per photon [31], respectively. The systematic uncertainties from the branching fraction of π^0 and η decays are taken from the PDG [23]. These sources of systematic uncertainty, which are summarized in the top part of Table II, are common for e^+e^- and $\mu^+\mu^-$ modes. The following sources of systematic uncertainty, which are uncorrelated for the e^+e^- and $\mu^+\mu^-$ modes, are summarized in the bottom part of Table II. The systematic

TABLE I. Results on $e^+e^- \to J/\psi\eta\pi^0$. Listed in the table are the integrated luminosity $\mathcal{L}$, radiative correction factor $(1+\delta^r)$ taken from QED calculation assuming the $Y(4260)$ cross section follows a Breit–Wigner line shape, vacuum polarization factor $(1+\delta^v)$, average efficiency $(\epsilon^{ee}\mathcal{B}^{ee}+\epsilon^{\mu\mu}\mathcal{B}^{\mu\mu})$, number of observed events $N^{\rm obs}$, number of estimated background events $N^{\rm bkg}$, the efficiency corrected upper limits on the number of signal events $N^{\rm up}$, and upper limits on the Born cross section $\sigma_{\rm UL}^{\rm Born}$ (at the 90% C.L.) at each energy point.

$\sqrt{s}$ (GeV)	$\mathcal{L}$(pb^{-1})	$(1+\delta^r)$	$(1+\delta^v)$	$(\epsilon^{ee}\mathcal{B}^{ee}+\epsilon^{\mu\mu}\mathcal{B}^{\mu\mu})$ (%)	$N^{\rm obs}$	$N^{\rm bkg}$	$N^{\rm up}$	$\sigma_{\rm UL}^{\rm Born}$ (pb)
4.009	482.0	0.838	1.044	2.1 ± 0.1(sys)	5	1	598.1	3.6
4.226	1047.3	0.844	1.056	2.2 ± 0.1(sys)	12	11	592.9	1.7
4.257	825.6	0.847	1.054	2.2 ± 0.1(sys)	12	8	654.1	2.4
4.358	539.8	0.942	1.051	2.2 ± 0.1(sys)	5	4	283.2	1.4
4.416	1028.9	0.951	1.053	2.3 ± 0.1(sys)	5	6	342.7	0.9
4.599	566.9	0.965	1.055	2.4 ± 0.1(sys)	6	3	418.4	1.9

TABLE II. Systematic uncertainties in the $J/\psi\eta\pi^0$ cross section measurement at each energy point (in %). The items in parentheses in the bottom part of the table are the uncorrelated systematic uncertainties for the e^+e^- (first) and $\mu^+\mu^-$ (second) modes.

Sources/$\sqrt{s}$ (GeV)	4.009	4.226	4.257	4.358	4.416	4.599
Luminosity	1.0	1.0	1.0	1.0	1.0	1.0
MDC tracking	2.0	2.0	2.0	2.0	2.0	2.0
Photon reconstruction	4.0	4.0	4.0	4.0	4.0	4.0
$\mathcal{B}(\pi^0\to\gamma\gamma)$, B$(\eta\to\gamma\gamma)$	0.5	0.5	0.5	0.5	0.5	0.5
$\mathcal{B}(J/\psi\to l^+l^-)$	(0.5, 0.5)	(0.5, 0.5)	(0.5, 0.5)	(0.5, 0.5)	(0.5, 0.5)	(0.5, 0.5)
MUC hits	(0, 3.6)	(0, 3.6)	(0, 3.6)	(0, 3.6)	(0, 3.6)	(0, 3.6)
J/ψ mass resolution	(0.2, 1.3)	(0.8, 1.2)	(0.5, 1.3)	(0.2, 0.7)	(0.7, 1.6)	(0.1, 0.6)
Decay model	(1.5, 1.9)	(0.9, 1.1)	(0.4, 0.6)	(0.2, 0.7)	(0.7, 0.2)	(0.2, 0.2)
Kinematic fitting	(1.2, 0.9)	(1.1, 1.2)	(0.9, 0.9)	(0.7, 1.2)	(1.1, 1.0)	(1.0, 1.4)
Total	5.3	5.3	5.2	5.2	5.3	5.2

uncertainty from the branching fraction of J/ψ decay is taken from the PDG [23]. The systematic uncertainty from the requirement on the number of MUC hits is 3.6% and estimated by comparing the efficiency of the MUC requirement between data and MC in the control sample $e^+e^- \to \pi^0\pi^0 J/\psi$ at $\sqrt{s}=4.257$ GeV. The systematic uncertainty from the requirement of the J/ψ signal region is estimated by smearing the invariant mass of l^+l^- of the signal MC with a Gaussian function to compensate for the resolution difference between the data and MC when calculating the efficiency. The parameters for smearing are determined by fitting the J/ψ distribution of data with the MC shape convoluted with a Gaussian function for the control sample $e^+e^- \to \pi^0\pi^0 J/\psi$. The difference in the detection efficiency between signal MC samples with and without the smearing is taken as the systematic uncertainty. The systematic uncertainty from the MC model is estimated by generating a MC sample with the angular distribution of leptons determined from the $\pi^+\pi^- J/\psi$ data. The systematic uncertainty due to kinematic fitting is estimated by correcting the helix parameters of charged tracks according the method described in Ref. [32], where the correction factors are obtained from the control sample $\psi' \to \gamma\chi_{cJ}$ and the difference in the detection efficiency between with and without making the correction to the MC is taken as the systematic uncertainty. The uncorrelated systematic uncertainties for the electron and muon channels are combined by taking the weighted average with weights $\epsilon^{ee}\mathcal{B}^{ee}$ and $\epsilon^{\mu\mu}\mathcal{B}^{\mu\mu}$, respectively. The total systematic uncertainty is obtained by summing all the sources of the systematic uncertainty in quadrature.

The systematic uncertainty on the size of the background is estimated by evaluating $N^{\rm up}$ with different signal and sideband regions for η and π^0. The most conservative $N^{\rm up}$ is taken as the final result, as listed in Table I. The upper limits on the Born cross section of $e^+e^- \to J/\psi\eta\pi^0(\sigma_{\rm UL}^{\rm Born})$ assuming it follows a $Y(4260)$ Breit–Wigner line shape are listed in Table I.

For comparison, the radiative correction factor and detection efficiency have been recalculated assuming the $e^+e^- \to J/\psi\eta\pi^0$ cross section follows alternative line shapes. If the cross section follows the line shape of the $Y(4040)$, the upper limit on the Born cross section is 4.1 pb at $\sqrt{s}=4.009$ GeV. For a $Y(4360)$ line shape, it is 1.6 pb at $\sqrt{s}=4.358$ GeV. For a $Y(4415)$ line shape, it is

1.5 pb at $\sqrt{s} = 4.358$ GeV and 1.0 pb at $\sqrt{s} = 4.416$ GeV. For a $Y(4660)$ line shape, it is 2.0 pb at $\sqrt{s} = 4.599$ GeV.

It is also possible to set upper limits on $e^+e^- \to Z_c^0\pi^0 \to J/\psi\eta\pi^0$. The number of observed events and number of estimated background events in the Z_c^0 signal region ($3.850 < M(J/\psi\eta) < 3.940$ GeV/c^2) are 7 and 4 ± 2, respectively, at $\sqrt{s} = 4.226$ GeV, and 8 and 3 ± 2, respectively, at $\sqrt{s} = 4.257$ GeV. The upper limit on $\sigma(e^+e^- \to Z_c^0\pi^0 \to J/\psi\eta\pi^0)$ is determined to be 1.3 pb at $\sqrt{s} = 4.226$ GeV and 2.0 pb at $\sqrt{s} = 4.257$ GeV, where only the statistical uncertainty is given. Compared to the measured cross section of $e^+e^- \to Z_c^0\pi^0 \to J/\psi\pi^0\pi^0$ [33], the upper limit on the ratio of the branching fraction $\frac{\mathcal{B}(Z_c^0\to J/\psi\eta)}{\mathcal{B}(Z_c^0\to J/\psi\pi^0)}$ at the 90% confidence level is 0.15 at $\sqrt{s} = 4.226$ GeV and 0.65 at $\sqrt{s} = 4.257$ GeV.

V. SUMMARY

In summary, using data collected with the BESIII detector, a search for the isospin violating decay $Y(4260) \to J/\psi\eta\pi^0$ is performed. No statistically significant signal is observed. The Born cross sections of $e^+e^- \to J/\psi\eta\pi^0$ at the 90% confidence level limits at $\sqrt{s} = 4.009$, 4.226, 4.257, 4.358, 4.416, and 4.599 GeV are determined to be 3.6, 1.7, 2.4, 1.4, 0.9, and 1.9 pb, respectively. The upper limits are well above the prediction for the molecule model [18].

ACKNOWLEDGMENTS

The BESIII Collaboration thanks the staff of BEPCII and the IHEP computing center for their strong support. This work is supported in part by National Key Basic Research Program of China under Contract No. 2015CB856700; National Natural Science Foundation of China (NSFC) under Contracts No. 11125525, No. 11235011, No. 11322544, No. 11335008, and No. 11425524; the Chinese Academy of Sciences (CAS) Large-Scale Scientific Facility Program; Joint Large-Scale Scientific Facility Funds of the NSFC and CAS under Contracts No. 11179007, No. U1232201, and No. U1332201; CAS under Contracts No. KJCX2-YW-N29 and No. KJCX2-YW-N45; 100 Talents Program of CAS; INPAC and Shanghai Key Laboratory for Particle Physics and Cosmology; German Research Foundation DFG under Contract No. Collaborative Research Center CRC-1044; Istituto Nazionale di Fisica Nucleare, Italy; Ministry of Development of Turkey under Contract No. DPT2006K-120470; Russian Foundation for Basic Research under Contract No. 14-07-91152; US Department of Energy under Contracts No. DE-FG02-04ER41291, No. DE-FG02-05ER41374, No. DE-FG02-94ER40823, and No. DESC0010118; US National Science Foundation; University of Groningen and the Helmholtzzentrum fuer Schwerionenforschung GmbH, Darmstadt; and the WCU Program of National Research Foundation of Korea under Contract No. R32-2008-000-10155-0.

[1] B. Aubert *et al.* (*BABAR* Collaboration), Phys. Rev. Lett. **95**, 142001 (2005).
[2] G. Pakhlova *et al.* (Belle Collaboration), Phys. Rev. Lett. **98**, 092001 (2007).
[3] L. Maiani, V. Riquer, F. Piccinini, and A. D. Polosa, Phys. Rev. D **72**, 031502 (2005).
[4] G. J. Ding, Phys. Rev. D **79**, 014001 (2009).
[5] S. L. Zhu, Phys. Lett. B **625**, 212 (2005).
[6] C. F. Qiao, Phys. Lett. B **639**, 263 (2006).
[7] M. Ablikim *et al.* (BESIII Collaboration), Phys. Rev. Lett. **110**, 252001 (2013).
[8] Z. Q. Liu *et al.* (Belle Collaboration), Phys. Rev. Lett. **110**, 252002 (2013).
[9] T. Xiao, S. Dobbs, A. Tomaradze, and K. K. Seth, Phys. Lett. B **727**, 366 (2013).
[10] Q. Wang, C. Hanhart, and Q. Zhao, Phys. Rev. Lett. **111**, 132003 (2013).
[11] M. Ablikim *et al.* (BESIII Collaboration), arXiv:1503.03408.
[12] K. Abe *et al.* (Belle Collaboration), arXiv:hep-ex/0505037.
[13] P. del Amo Sanchez *et al.* (*BABAR* Collaboration), Phys. Rev. D **82**, 011101 (2010).
[14] M. B. Voloshin, Phys. Rev. D **86**, 034013 (2012).
[15] A. Ali, C. Hambrock, and M. J. Aslam, Phys. Rev. Lett. **104**, 162001 (2010).
[16] A. Ali, C. Hambrock, and S. Mishima, Phys. Rev. Lett. **106**, 092002 (2011).
[17] L. Maiani, V. Riquer, R. Faccini, F. Piccinini, A. Pilloni, and A. D. Polosa, Phys. Rev. D **87**, 111102 (2013).
[18] X. G. Wu, C. Hanhart, Q. Wang, and Q. Zhao, Phys. Rev. D **89**, 054038 (2014).
[19] M. Ablikim *et al.* (BESIII Collaboration), Nucl. Instrum. Methods Phys. Res., Sect. A **614**, 345 (2010).
[20] S. Agostinelli *et al.* (GEANT4 Collaboration), Nucl. Instrum. Methods Phys. Res., Sect. A **506**, 250 (2003).
[21] Z. Y. Deng *et al.*, High Energy Phys. Nucl. Phys. **30**, 371 (2006).
[22] S. Jadach, B. F. L. Ward, and Z. Was, Comput. Phys. Commun. **130**, 260 (2000); Phys. Rev. D **63**, 113009 (2001).
[23] K. A. Olive *et al.* (Particle Data Group Collaboration), Chin. Phys. C **38**, 090001 (2014).
[24] P. Golonka and Z. Was, Eur. Phys. J. C **45**, 97 (2006).
[25] D. J. Lange, Nucl. Instrum. Methods Phys. Res., Sect. A **462**, 152 (2001).
[26] R. G. Ping, Chin. Phys. C **32**, 599 (2008).
[27] T. Sjöstrand *et al.*, arXiv:hep-ph/0108264.

[28] S. Actis *et al.*, Eur. Phys. J. C **66**, 585 (2010).
[29] W. Rolke, A. Lopez, J. Conrad, and F. James, Nucl. Instrum. Methods Phys. Res., Sect. A **551**, 493 (2005).
[30] M. Ablikim *et al.* (BESIII Collaboration), Phys. Rev. Lett. **112**, 022001 (2014).
[31] M. Ablikim *et al.* (BESIII Collaboration), Phys. Rev. D **83**, 112005 (2011).
[32] M. Ablikim *et al.* (BESIII Collaboration), Phys. Rev. D **87**, 012002 (2013).
[33] M. Ablikim *et al.* (BESIII Collaboration), arXiv:1506.06018.